

Creep of organic soils due to small load increments

Fluage des sols organiques dû à de faibles augmentations de charge

C. Zwanenburg*

Deltares – Delft University of Technology, Delft, The Netherlands

B. Wittekoek, M. Konstadinou
Deltares, Delft, The Netherlands

*cor.zwanenburg@deltares.nl

ABSTRACT: Organic soils are susceptible to creep. When predicting settlement of organic deposits due to small load increments, the initial conditions, particularly the initial strain rate should be assessed carefully. Recent developments in predicting creep behaviour of clays are tested in an ongoing study on organic soil behaviour. A series of incremental loading tests on peat and organic clay shows that a framework of undisturbed isotachs cannot be used to predict strain rates in over-consolidated conditions. This complicates the applicability of conventional incremental loading test results for assessing field conditions. Additionally, the tests show the relevance of a large strain approach when dealing with soft organic soils.

RÉSUMÉ: Les sols organiques sont susceptibles de fluer. Lors de la prévision du tassement des dépôts organiques dû à de faibles incréments de charge, les conditions initiales, en particulier la vitesse de déformation initiale, doivent être évaluées avec soin. Les développements récents dans la prévision du comportement au fluage des argiles sont testés dans une étude en cours sur le comportement des sols organiques. Une série d'essais de chargement incrémentiel sur tourbe et argile organique montre qu'un cadre d'isotaches non perturbés ne peut pas être utilisé pour prédire les taux de déformation dans des conditions sur-consolidées. Cela complique l'applicabilité des résultats des tests de chargement incrémentiels conventionnels pour évaluer les conditions sur le terrain. De plus, les tests montrent la pertinence d'une approche à grandes déformations lorsqu'il s'agit de sols organiques mous.

Keywords: Settlement; creep; organic soils.

1 INTRODUCTION

Organic soils are known for their tendency to creep. Yet, most 1D creep theories are typically derived for clays. This paper discusses some results of a study that examines the applicability of the 1D creep theories for organic soils.

This study focusses on small load increments. These are increments for which the soil stress remains below the yield stress. For predicting creep due to small load increments, the initial conditions, such as strain rate prior to loading, play an important role.

2 TESTED MATERIAL

Two material types are selected for testing: peat sampled at Zegveld and an organic clay sampled near Bleskensgraaf, The Netherlands. Table 1 and Table 2 present the characteristics of the tested materials.

The material was sampled by the DLDS sampler. This sampler takes block samples, 400 mm in diameter and 500 mm in height. Details of the sampler are given by Zwanenburg (2017).

Table 1. Characteristics of the tested peat samples.

sample	Depth [m]	W [%]	γ [kN/m ³]
25	-3.90	673	9.41
26	-3.90	675	9.34
42	-7.48	830	9.13
55	-3.13	578	9.80
65	-7.71	843	9.60
67	-3.42	420	9.40
97	-3.42	585	9.58
99	-3.31	656	9.02
9	-2.93	587	9.57

Table 2. Characteristics of the tested organic clay samples.

sample	Depth [m]	W [%]	γ [kN/m ³]
1	-3.04	62	15.2
2	-3.04	118	13.0

The volumetric weights indicate that the samples might be unsaturated, which is explained by the presence of gas in the peat deposits. As indicated by Persekian (2011), the gas content might run up to 30%. The organic content of the tested peat samples is in the order of 79%.

The organic clay samples show natural heterogeneity, as shown by the water content, W and

volume weight, γ . The organic content of the clay is in the order of 3.6% for test 1 and 6.5% for test 2.

3 THEORY

This study follows the isotach frame as discussed by Leroueil (2006), Yin & Graham (1989), Den Haan (1992, 1999), Den Haan & Edil (1994), Leroueil et al. (1985).

The 1D creep compression and creep rate follows from:

$$\varepsilon_c = C_\alpha \log\left(\frac{\tau}{\tau_0}\right), \dot{\varepsilon}_c = \frac{C_\alpha}{2.3\tau} \quad (1)$$

in which, ε_c represents linear strain due to creep, $\dot{\varepsilon}_c$ creep strain rate, C_α creep parameter, τ intrinsic time and τ_0 reference intrinsic time, $\tau_0 = 1$ day. With intrinsic time, τ as the time scale for soil deformation related to the isotach field, Den Haan (1992, 1999).

The relation between changes in intrinsic time and load steps follows from:

$$\tau_i = \tau_{i-1} \left(\frac{\sigma'_{i-1}}{\sigma'_i}\right)^{\frac{CR-RR}{C_\alpha}} \quad (2)$$

in which τ_i and τ_{i-1} represent the different intrinsic time values in the different load steps, σ'_i , σ'_{i-1} the effective stresses during these steps, CR the compression ratio and RR the recompression ratio.

For specific stress conditions, the intrinsic time can be found by Equation (2). When referring to the 1-day compression line, $\tau_{i-1} = 1$ day, σ'_{i-1} is the yield stress, σ'_{vy} and OCR = over-consolidation ratio, Equation (2) turns into:

$$\tau = OCR \frac{CR-RR}{C_\alpha} \quad (3)$$

Recent developments (Yuan & Whittle, 2018) allow for a constant or non-constant spacing between the isotachs by introducing a parameter β . For $\beta = C_\alpha/(CR-RR)$, the Yuan & Whittle model aligns with Eq. (2). Smaller values for β mimic the conditions of reducing distance between the isotachs. The Yuan & Whittle model also introduces an activation of creep on changes in loading.

Vergote (2020) describes non-linear isotachs caused by structural changes due to unloading. Disturbed isotachs will lead to larger strain rates on unloading compared to the undisturbed isotachs.

4 TEST SET UP

In total 9 incremental loading tests, IL, have been conducted on peat and 2 IL tests on the organic clay. The applied loading scheme is given in Figure 1. Additional testing, including constant rate of strain, CRS testing is still ongoing.

The tests use a WILLE oedometer test set-up. A 1 kN load cell provides the load measurement. An LVDT is placed directly on the top cap to measure vertical displacements. The initial sample height, h_0 , was 20 mm for the peat samples and 30 mm for the organic clay samples.

To validate Equations (1) and (2), the tests include multiple loading and unloading steps. The duration of the different load steps is 24 hours except for the steps 2 and 10 which were extended to 168 hours (1 week). This loading scheme allows to determine the relevant parameters from the conventional 24 h loading steps to examine the creep strain and strain rate for the 168-hours steps. In this way parameters are derived and applied in the analysis of the same test, eliminating the possible effect of heterogeneity between the samples. For the organic clay tests only 24 hours load steps were applied. After the unloading step, multiple loading steps with reducing OCR have been applied. This allows for examining the influence of OCR on the calculated and observed strain rates.

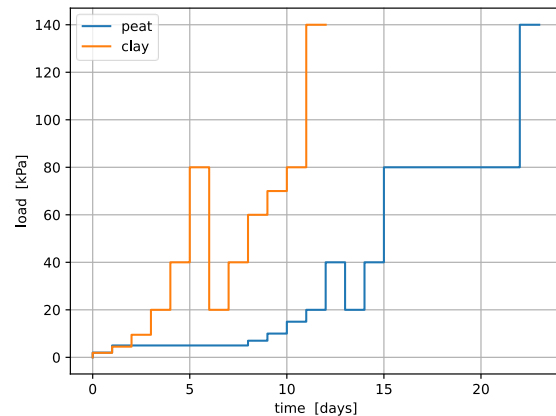


Figure 1. Applied loading schemes.

5 RESULTS TESTED PEAT SAMPLES

Figure 2 shows some results for test 25, which are considered typical for the tests on peat.

Table 3 shows that the ratio $(CR-RR)/C_\alpha$ ranges from 8.3 to 19.7 for the tested peat and 11 to 23 for the tested organic clay, see Table 5. Consequently, the relation between load increments and intrinsic time increments is highly non-linear and small deviations in for example OCR in Eq. (3) has a strong influence on the calculated intrinsic time.

The 1-day compression line, Figure 2a, starts to bend at $\epsilon_a > 0.4$. This is explained by the finite layer thickness and can be addressed by using a large strain approach (Den Haan, 1999). The strain rate in step 2, with a vertical load of 5 kPa and representing OC conditions is clearly lower than found in step 10, with a vertical load of 80 kPa, representing NC conditions.

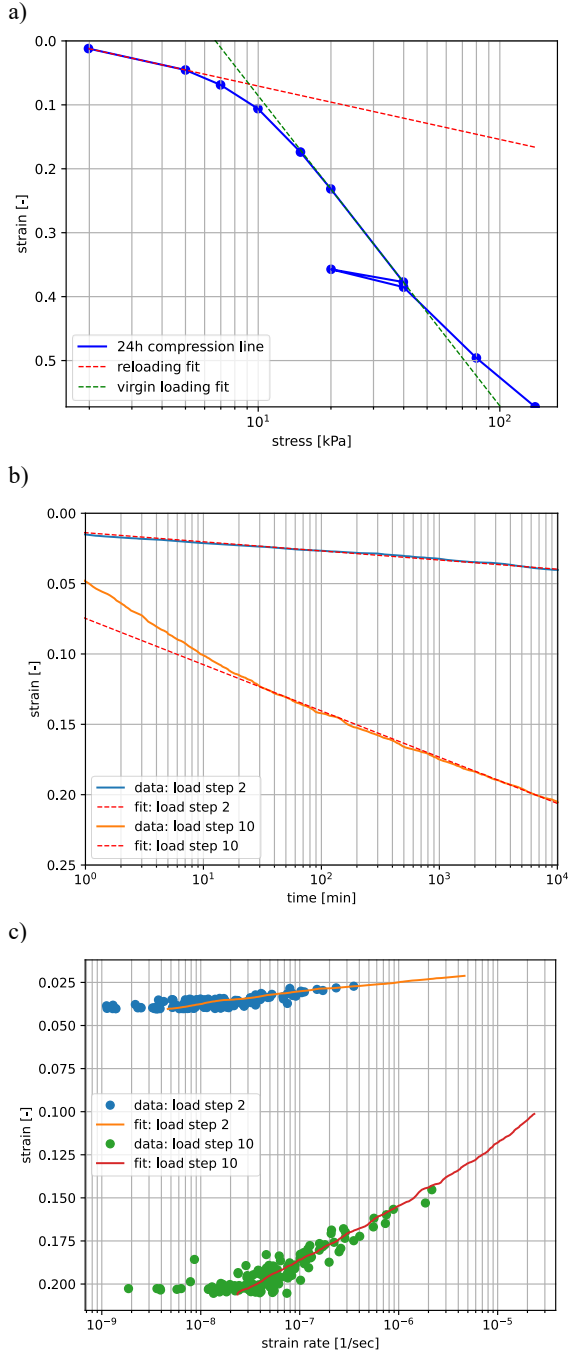


Figure 2. Results of test 25, a) 24h compression curve, b) time – strain development for load steps 2 and 10, c) strain rate – strain development for load steps 2 and 10.

Table 3. Comparison between calculated and measured creep strain rate at the end of step 2, $OCR_2 = OCR$ in step 2, $C_{\alpha,10} = C_{\alpha}$ derived from step 10.

nr	(CR-RR) / C_{α}	$C_{\alpha,10}$	OCR_2	$\epsilon_{cal} \times 10^{-9}$ [1/s]*	$\epsilon_m \times 10^{-9}$ [1/s]
25	12.7	0.0329	1.8	0.073	4.6
26	13.4	0.0315	2.1	0.0084	3.2
42	15.9	0.0303	2.7	0.00003	2.1
55	19.7	0.0309	3.1	4.0×10^{-8}	1.0
65	10.7	0.0344	2.3	0.03	4.6
67	8.8	0.0374	2.2	0.21	8.8
97	8.7	0.0372	2.2	0.2	7.4
99	8.3	0.0429	1.8	1.5	13
9	11.2	0.0391	2.5	0.0074	3.2

*Calculated using Equation (1).

Table 3 summarizes the results. The creep parameter is evaluated from step 10, $C_{\alpha,10}$, by curve fitting, as indicated by the red dotted line in Figure 2b. The curve fitting yields $\mu_{C_{\alpha}} = 0.035$ with coefficient of variation, COV = 0.12. The OCR in step 2 fluctuates around 2.3.

Figure 2a shows the curve fitting of the compression line providing the RR and CR values, which are combined with $C_{\alpha,10}$ to obtain (CR-RR) / C_{α} values as presented by Table 3.

The last column in Table 3 presents the measured creep strain rates found at the end of loading phase 2. The obtained values are in the order of 10^{-9} to 10^{-8} 1/s. Using Eq. (1), the strain rates are assessed for the same test phase. The calculated values, column 5 of Table 3, show a large variety and clearly underpredict the measured values. Small changes in (CR-RR) / C_{α} cannot explain the differences.

Using ϵ_m^* , Eq. (1) and (3) yield an effective OCR, OCR_{eff} , which corresponds to the observed strain rates. Table 4 compares OCR_{eff} and OCR. On average, OCR_{eff} is 62% of OCR.

Table 4. Comparison of OCR_{eff} and applied OCR

nr	OCR_{eff}	OCR_2	OCR_{eff}/OCR_2
25	1.33	1.8	0.74
26	1.34	2.1	0.64
42	1.31	2.7	0.48
55	1.29	3.1	0.42
65	1.40	2.3	0.61
67	1.42	2.2	0.64
97	1.45	2.2	0.66
99	1.40	1.8	0.78
9	1.44	2.5	0.58

It should be noted that for normally consolidated conditions, step 10, the calculated and measured strain rates are in good agreement. This is visualised by test 25. For $C_{\alpha} = 0.0329$, see Table 3, and $\tau = 10^4$ min (6×10^5 sec), Eq. (1) gives $\epsilon_{cal}^* = 2.4 \times 10^{-8}$ 1/s, which

corresponds nicely to the measured creep strain rate at the end of loading stage 10 in Figure 2c.

6 RESULTS ORGANIC CLAY

Figure 3 shows the compression curve as a function of void ratio for the two oedometer tests on organic clay. Table 6 shows a good agreement between the measured and calculated strain rates for normally consolidated conditions. For over-consolidated conditions, however, the measured strain rate decreases mildly whereas the calculated strain rate is orders in magnitude smaller. It should be noted that when including a reducing C_α , the calculated strain rates would reduce even stronger for increasing OCR.

Table 5. re-compression ratio, RR, compression ratio, CR, creep parameter C_α and yield stress σ'_{vy} for oedometer test 1 and 2.

Test	RR	CR	C_α	(CR-RR)/ C_α	σ'_{vy} [kPa]
1	0.011	0.16	0.0065	22.9	14
2	0.025	0.29	0.025	10.6	22

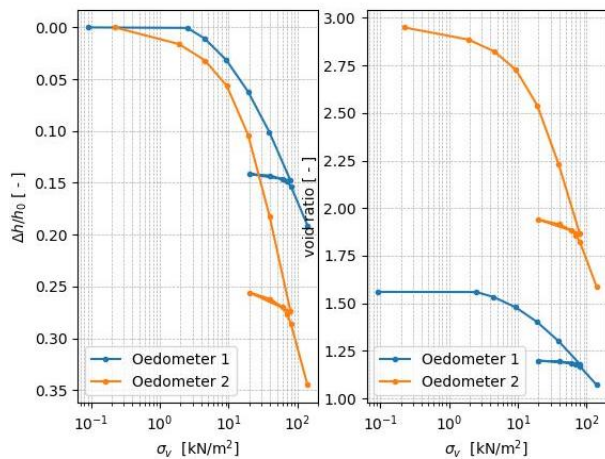


Figure 3. 24h compression curves, left) stress vs strain rate, right) stress vs void ratio, e.

Table 6. Results for Test 1 and 2 on organic clay

Step nr	OCR		$\dot{\epsilon}_m$ [1/s] $\times 10^{-8}$		$\dot{\epsilon}_c$ [1/s]*	
	1	2	1	2	1	2
2	4.5	4.4	0.15	1.5	3.4×10^{-23}	1.8×10^{-14}
3	2.2	2.1	0.7	2.5	6.6×10^{-16}	4.2×10^{-11}
4	1.0	1.0	2.8	5.7	0.8×10^{-8}	4.8×10^{-8}
5	1.0	1.0	2.27	11.8	1.5×10^{-8}	6.1×10^{-8}
6	1.0	1.0	3.3	19.3	1.5×10^{-8}	6.1×10^{-8}
8	2.0	2.0	0.07	0.37	5.2×10^{-15}	8.9×10^{-11}
9	1.3	1.3	0.32	0.31	5.6×10^{-11}	6.2×10^{-9}
10	1.1	1.1	0.26	1.9	0.2×10^{-8}	2.6×10^{-8}
11	1.0	1.0	0.57	4.6	1.5×10^{-8}	6.2×10^{-8}
12	1.0	1.0	3.60	11.7	1.5×10^{-8}	6.1×10^{-8}

*Calculated using Equation (1).

7 CONCLUSIONS

The tests on peat and organic clay show the same tendency. Calculated creep strain rates for normally consolidated conditions correspond to the measured creep strain rates. For over-consolidated conditions, however, calculations following Den Haan (1992, 1999) underpredict the creep strain rates. The difference between the measured and calculated creep strain rates increases for increasing OCR.

A reducing C_α with OCR does not improve the calculations. Instead, disturbed isotachs (Vergote 2020), might provide a framework within which an explanation for this behaviour could be found. This will be part of a follow-up study.

The tests on organic clay show that the difference between the measured and predicted strain rate is found for both, the initial re-loading steps below the natural yield stress as well as for the re-loading steps in the second part of the test. In the field, initial strain rates are induced typically by long term creep or aging and unloading might not be relevant field conditions. This difference in stress conditions between field and incremental loading tests results in a difficulty for the assessment of the initial creep strain rate in the field.

The last loading steps, in the tests on peat, show an increase in stiffness, which is explained by the finite layer thickness. This shows the relevance for a large strain approach when dealing with organic soils.

REFERENCES

- Den Haan E.J. (1992) The formulation of virgin compression of soils *Géotechnique*, vol 42, p 465-483 DOI: 10.1680/geot.1992.42.3.465
- Den Haan E.J., Edil T.B. (1994) Secondary and tertiary compression of peat in: *Advances in understanding and modelling the mechanical behaviour of peat*, den Haan, Termaat & Edil (eds), Balkema Rotterdam
- Den Haan E.J. (1999) Stress independent parameters for primary and secondary compression in: *Proceedings XIIIth International Conference on Soil Mechanics and Foundation Engineering*, New Delhi, Vol I, p 65 – 70
- Leroueil S., Kabbaj M., Tavenas F., Bouchard R. (1985). Stress-strain-strain rate relation for the compressibility of sensitive natural soils *Géotechnique* 35(2) 159-180 doi:/10.1007/978-3-642-32814-5_15
- Leroueil S. (2006) The isotach approach. Where are we 50years after its development by Professor Šuklje? in: *Proceedings of the 13th Danube-European Conference on Geotechnical Engineering, Prof. Suklje's memorial lecture*, Ljubljana 2006 pp 55-88
- Persekian A.D. (2011). *Geophysical estimation of free-phase gas content and distribution in peatlands PhD Thesis* State University of New Jersey
- Vergote T.A. (2020). *Deformation of soils: time and strain effects after unloading* PhD thesis National University

Singapore.

Downloadable:

<https://scholarbank.nus.edu.sg/handle/10635/185992>

Yin J.-H., Graham J. (1989). Viscous-elastic-plastic modelling of one-dimensional time-dependant behaviour of clays *Canadian Geotechnical Journal* **26** 199-209, doi.org/10.1139/t89-029

Yuan, Y., & Whittle, A.J. (2018). A novel elasto-viscoplastic formulation for compression behaviour of clays. *Géotechnique* **68**(12), 1044, doi: 10.1680/jgeot.16.P276

Zwanenburg C. (2017). The development of a large diameter sampler in: *proc. 19th international conference on soil mechanics and geotechnical engineering*, Seoul

B - Geohazards
B - Géorisques

INTERNATIONAL SOCIETY FOR SOIL MECHANICS AND GEOTECHNICAL ENGINEERING



This paper was downloaded from the Online Library of the International Society for Soil Mechanics and Geotechnical Engineering (ISSMGE). The library is available here:

<https://www.issmge.org/publications/online-library>

This is an open-access database that archives thousands of papers published under the Auspices of the ISSMGE and maintained by the Innovation and Development Committee of ISSMGE.

The paper was published in the proceedings of the 18th European Conference on Soil Mechanics and Geotechnical Engineering and was edited by Nuno Guerra. The conference was held from August 26th to August 30th 2024 in Lisbon, Portugal.